Structural Changes of the Sarcoplasmic Reticulum Ca2+−ATPase upon Nucleotide Binding Studied by Fourier Transform Infrared Spectroscopy

ARTICLE *in* BIOPHYSICAL JOURNAL · APRIL 2000

Impact Factor: 3.97 · DOI: 10.1016/S0006-3495(00)76705-1 · Source: PubMed

3 AUTHORS, INCLUDING:

Andreas Barth
Stockholm University
96 PUBLICATIONS **3,746** CITATIONS
SEE PROFILE

Werner Mäntele
Goethe-Universität Frankfurt am Main
131 PUBLICATIONS **3,562** CITATIONS
SEE PROFILE

Structural Changes of the Sarcoplasmic Reticulum Ca^{2+}-ATPase upon Nucleotide Binding Studied by Fourier Transform Infrared Spectroscopy

Frithjof von Germar, Andreas Barth, and Werner Mäntele
Institut für Biophysik, Johann Wolfgang Goethe Universität Frankfurt, D-60590 Frankfurt am Main, Germany

ABSTRACT Changes in the vibrational spectrum of the sarcoplasmic reticulum Ca^{2+}-ATPase upon nucleotide binding were recorded in H_2O and ^2H_2O at −7°C and pH 7.0. The reaction cycle was triggered by the photochemical release of nucleotides (ATP, ADP, and AMP-PNP) from a biologically inactive precursor (caged ATP, P^3-1-(2-nitrophenyl) adenosine 5′-triphosphate, and related caged compounds). Infrared absorbance changes due to ATP release and two steps of the Ca^{2+}-ATPase reaction cycle, ATP binding and phosphorylation, were followed in real time. Under the conditions used in our experiments, the rate of ATP binding was limited by the rate of ATP release ($k_{app} \cong 3\ s^{-1}$ in H_2O and $k_{app} \cong 7\ s^{-1}$ in ^2H_2O). Bands in the amide I and II regions of the infrared spectrum show that the conformation of the Ca^{2+}-ATPase changes upon nucleotide binding. The observation of bands in the amide I region can be assigned to perturbations of α-helical and β-sheet structures. According to similar band profiles in the nucleotide binding spectra, ATP, AMP-PNP, and ADP induce similar conformational changes. However, subtle differences between ATP and AMP-PNP are observed; these are most likely due to the protonation state of the γ-phosphate group. Differences between the ATP and ADP binding spectra indicate the significance of the γ-phosphate group in the interactions between the Ca^{2+}-ATPase and the nucleotide. Nucleotide binding affects Asp or Glu residues, and bands characteristic of their protonated side chains are observed at 1716 cm^{-1} (H_2O) and 1706 cm^{-1} (^2H_2O) and seem to depend on the charge of the phosphate groups. Bands at 1516 cm^{-1} (H_2O) and 1514 cm^{-1} (^2H_2O) are tentatively assigned to a protonated Tyr residue affected by nucleotide binding. Possible changes in Arg, Trp, and Lys absorption and in the nucleoside are discussed. The spectra are compared with those of nucleotide binding to arginine kinase, creatine kinase, and H-ras P21.

INTRODUCTION

Muscle contraction is triggered by an increase in the Ca^{2+} concentration in skeletal muscle cells. For relaxation, Ca^{2+} has to be transported back into the sarcoplasmic reticulum (SR) by the intrinsic membrane protein Ca^{2+}-ATPase, which couples active Ca^{2+} transport to ATP hydrolysis. The reaction cycle is shown in a simplified form in Fig. 1 (Andersen, 1989). The model for the reaction cycle by de Meis and Vianna (1979) is based on the assumption of two main functional conformational states, E_1 and E_2, of the protein. Two Ca^{2+} ions are bound to high-affinity binding sites from the cytoplasmic side of the membrane, which allows ATP to phosphorylate the enzyme (Ca_2E_1-P). The following transition from the E_1-P form of the phosphoenzyme to the E_2-P form is associated with a reorientation of the Ca^{2+}-binding sites from the cytoplasmic to the luminal side of the membrane and a decrease in the Ca^{2+}-binding constant by three orders of magnitude, which leads to Ca^{2+} release into the SR lumen. Hydrolytic cleavage of the phosphoenzyme E_2-P completes the reaction cycle (Andersen, 1989). This work focuses on the structural effects of nucleotide binding to the ATPase, which is not only an intermediate step in the reaction cycle but also serves regulatory purposes (Andersen, 1989).

The reaction cycle can be triggered using "caged" substrates that are biologically inactive, UV-sensitive substrate analogs and rapidly releasing the free, active substrate with a UV-light flash. In combination with the Fourier transform infrared (FTIR) technique it is possible to detect conformational changes in the polypeptide backbone, in single amino acid side chains, and in functional groups of the substrate. The first infrared investigations of the Ca^{2+}-ATPase were made at low time resolution, and ADP binding but not ATP binding could be investigated (Barth et al., 1994). Time resolution is greatly improved by using the rapid scan technique, with a time resolution of 65 ms. Thus spectra of sequential states of the protein can be obtained, as can kinetic traces of individual difference bands (Barth et al., 1996). In these measurements it was possible to observe the intermediate ATPase state, in which ATP is bound to the ATPase before the formation of the phosphoenzyme. The infrared spectra were analyzed in terms of the extent of net secondary structure change in individual reaction steps, which was found to be rather low for all reaction steps investigated. However, changes induced by nucleotide binding are as prominent as changes by phosphorylation and phosphoenzyme conversion (Barth et al., 1996).

To gain more insight into the structural implications of nucleotide binding, we have studied here changes in the vibrational spectrum of the SR Ca^{2+}-ATPase upon binding of ATP, ADP, and the nonhydrolyzable ATP analog AMP-PNP (adenylyl-imido-diphosphate). AMP-PNP contains an

Received for publication 7 June 1999 and in final form 26 October 1999.
Address reprint requests to Dr. Andreas Barth, Institut für Biophysik, Johann Wolfgang Goethe Universität Frankfurt, Theodor Stern Kai 7, Haus 74, D-60590 Frankfurt am Main, Germany. Tel.: 49-69-6301-6087; Fax: 49-69-6301-5838; E-mail: barth@biophysik.uni-frankfurt.de.

0006-3495/00/03/1531/10 $2.00

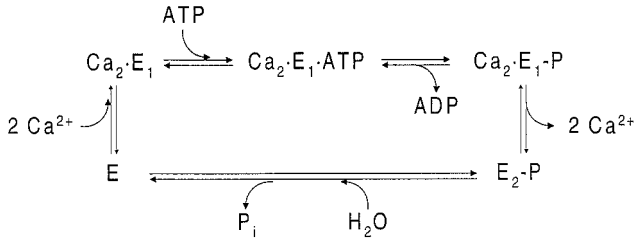

FIGURE 1 Simplified scheme of the reaction cycle (Andersen, 1989).

NH group between the β- and γ-phosphate groups instead of an oxygen, which is hydrolyzed only very slowly by the Ca^{2+}-ATPase (Taylor, 1981) and therefore does not allow accumulation of enzyme states in the reaction cycle beyond nucleotide binding.

MATERIALS AND METHODS

Sample preparation

SR vesicles were prepared as described (de Meis and Hasselbach, 1971). After overnight dialysis of these SR vesicles in H_2O or ^2H_2O buffer, IR samples were prepared by drying 10 μl of SR suspension onto a CaF_2 window with a trough of 5-μm depth and 8-mm diameter in a gentle stream of nitrogen and resuspending it immediately in 0.6 μl of 12% glycerol in H_2O or ^2H_2O. The sample was sealed with a second flat CaF_2 window and thermostatted at -7°C during the experiment. The samples contained ~1 mM Ca^{2+}-ATPase, ~0.5 mg/ml Ca^{2+}-ionophor A23187, ~2 mg/ml adenylate kinase, ~100 mM imidazole HCl (pH 7.0), ~100 mM KCl, and ~10 mM $CaCl_2$. Concentrations of the caged nucleotides and the number of experiments are listed in Table 1.

The ADP binding constant of SR Ca^{2+}-ATPase under the conditions of IR samples is smaller than for ATP, as shown by the higher ADP concentration needed to generate saturating protein signals. We thus doubled the concentration of caged ADP to maximize the amount of ADP bound to the Ca^{2+}-ATPase.

FTIR measurements

Measurements were carried out with a modified Bruker IFS 66 spectrometer equipped with a HgCdTe detector of selected sensitivity. Photolytic release of ATP, ADP, and AMP-PNP from their respective caged derivatives was triggered by a xenon flash tube (Barth et al., 1991). The flash energy was set to release ~2–3 mM ATP or AMP-PNP or ~4–6 mM ADP per flash. The concentration of the released nucleotide is thus two to six times higher than the ATPase concentration. Before the flash, one reference spectrum with 100 scans (I_0) was recorded. After the flash, 70 spectra were recorded, 30 spectra with one scan each, 20 spectra with two scans, and 20 spectra with 50 scans. Each scan consisted of one complete forward and backward mirror movement, taking 65 ms.

TABLE 1 Number of experiments and concentrations of different caged nucleotides

Nucleotide		Caged nucleotide concentration (mM)	No. of samples	No. of experiments
Caged ATP	H_2O	20	18	88
	^2H_2O	20	6	31
Caged AMP-PNP	H_2O	20	27	27
	^2H_2O	20	19	19
Caged ADP	H_2O	40	5	5
	^2H_2O	40	10	10
[^{15}N]Caged ATP	H_2O	20	6	30
	^2H_2O	20	6	28

Data processing

Difference spectra were directly obtained from spectra recorded from the same sample by calculating the ratio $-\log(I/I_0)$ from each spectrum after the flash (I) and the reference spectrum recorded before the flash (I_0). For a better comparison, difference spectra were normalized to equal protein content as described previously (Barth and Mäntele, 1998).

The spectra averaged between 1 and 2 s after the flash are characteristic of the nucleotide bound state of the protein but also show signals due to the photolysis reaction (see Results). Spectra of samples, prepared as described above with the same salt concentration but without protein, were recorded in the same time interval to obtain the "pure" photolysis spectra of the caged nucleotides. They were subtracted from the protein spectra, which results in the "pure" nucleotide binding spectra showing predominantly bands arising from nucleotide-protein interaction and, ideally, no photolysis signals. The subtraction factor was judged to be correct when the 1525 cm^{-1} region of the processed spectrum corresponded to that region in the spectrum obtained with [^{15}N]caged ATP. With this compound, because of labeling at the nitro position of the (2-nitrophenyl)ethyl-ester group, the 1525 cm^{-1} photolysis band shifts to 1499 cm^{-1}, which allows the identification of protein bands in the 1525 cm^{-1} region. As the released ATP is identical to that of the unlabeled caged ATP, the same interactions between the protein and the nucleotide are expected, and thus the spectrum obtained with [^{15}N]caged ATP can be used as a reference for a complete compensation for the 1525 cm^{-1} ν_{as} $^{14}NO_2$ band of the photolysis reaction.

AMP-PNP and ADP do not allow progression of the reaction cycle beyond the nucleotide-bound state at a significant rate, and the spectra recorded between 1 and 2 s and between 2 and 67 s are the same. For a better signal-to-noise ratio, the AMP-PNP and ADP binding spectra were calculated from the spectra obtained in the longer time interval.

For the kinetic analysis of ATP-induced difference spectra, selected bands showing the three partial reactions of nucleotide release, nucleotide binding, and phosphorylation were integrated as described previously (Barth et al., 1996). The fitting was done with the program Origin, and the kinetic constants obtained from the analysis of 20 (H_2O) or 17 (^2H_2O) bands were averaged.

RESULTS AND DISCUSSION

Interpretation of the kinetic data

Photolytic release of ATP from caged ATP in SR samples triggers the Ca^{2+}-ATPase reaction cycle. As observed earlier (Barth et al., 1996), in our samples containing 10 mM $CaCl_2$, the Ca_2E_1-P state accumulates, and three different reactions can be observed: photolytic release of ATP, ATP binding to the Ca^{2+}-ATPase, and ATPase phosphorylation. Kinetic analysis was performed at 20 different bands of the spectrum obtained with ATP in H_2O (Fig. 3 *A*) and 17 bands of the spectrum obtained with ATP in ^2H_2O (Fig. 4 *A*) to establish the optimum time interval for the observation of the ATPase intermediate with bound ATP, Ca_2E_1ATP. Marker bands characteristic of a specific reaction are shown in Fig. 2. Formation or decay of these bands reveals the rate constants of the respective reactions.

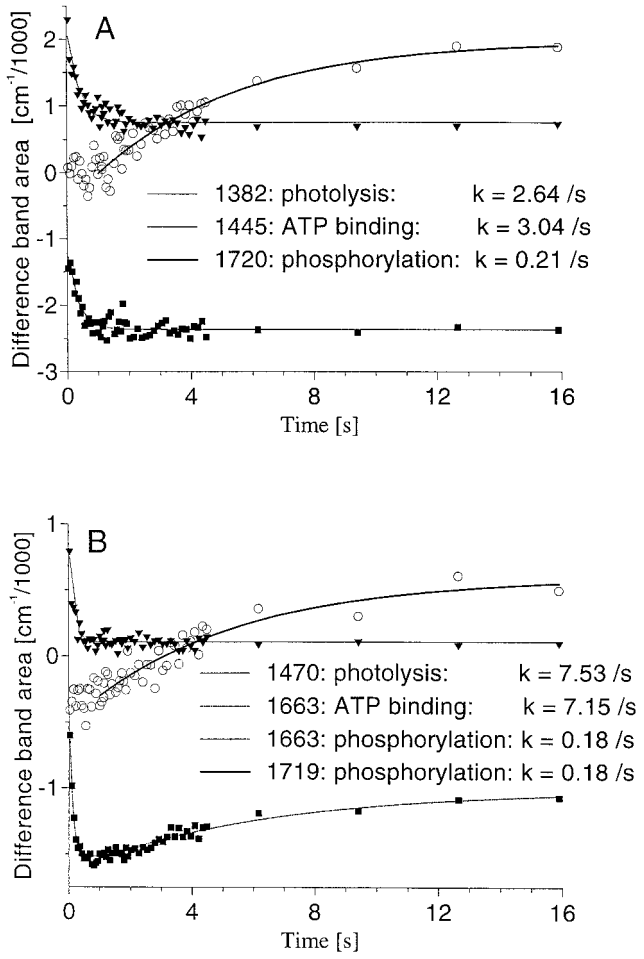

FIGURE 2 Kinetic traces of selected infrared bands in Ca^{2+}-ATPase samples with caged ATP. (*A*) Kinetics in H_2O monitoring photolysis (1382 cm^{-1} band, *closed triangles and thin line*), ATP binding (1445 cm^{-1} band, *closed squares and thin line*), and phosphorylation to form the E_1-P state (1720 cm^{-1} band, *open circles and bold line*). (*B*) Kinetics in ^2H_2O monitoring photolysis (1470 cm^{-1} band, *closed triangles and thin line*), phosphorylation to form the E_1-P state (1719 cm^{-1} band, *open circles and bold line*), and consecutive ATP binding and phosphorylation (1663 cm^{-1} band, *closed squares and thin line*). Photolysis of caged ATP was monitored with samples containing no Ca^{2+}-ATPase.

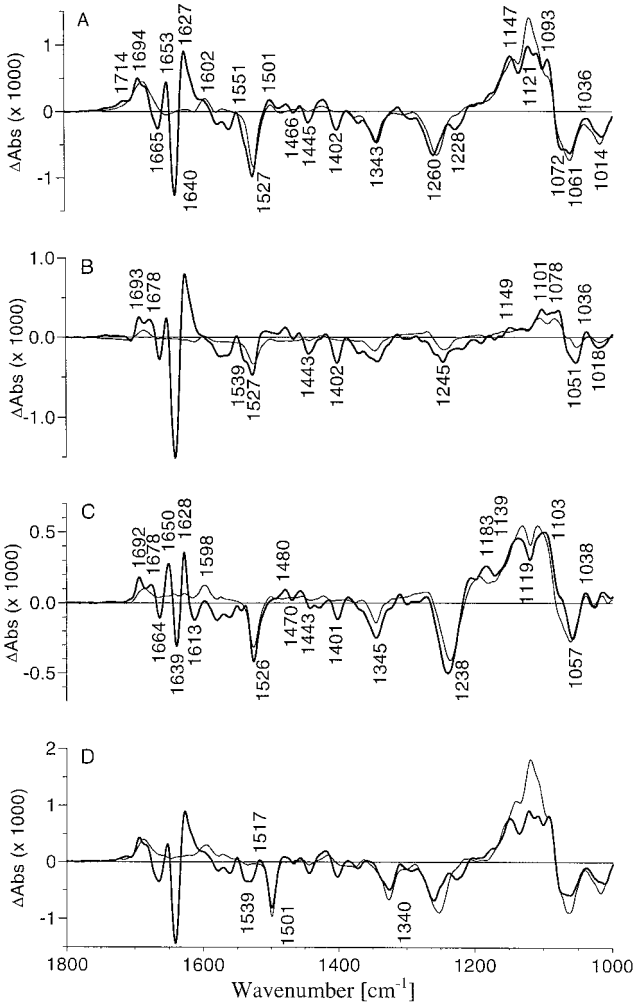

FIGURE 3 Infrared difference spectra upon nucleotide release in SR samples in H_2O at −7°C. *Bold line*: Spectra of nucleotide release in SR samples, showing the nucleotide binding state. *Thin line*: Photolysis spectra of the caged nucleotide. Labels refer to the spectra of SR samples. (*A*) Difference spectra obtained in samples containing caged ATP. (*B*) Difference spectra obtained with caged AMP-PNP. (*C*) Difference spectra obtained with caged ADP. (*D*) Difference spectra obtained with [^{15}N]caged ATP.

The release of ATP from caged ATP in H_2O is monitored best by the decay of the positive band at 1382 cm^{-1}, which is characteristic for the aci-nitro intermediate of caged ATP photolysis (Barth et al., 1997). Concomitant with the decay of this intermediate, ATP is released, which can therefore be monitored at 1382 cm^{-1}. The decay of this band was fitted with a single exponential rate constant of $k_{app} = 2.64\ s^{-1}$ (Fig. 2 *A*), which is consistent with data for the temperature dependency of caged ATP photolysis (Barth et al., 1997).

ATP binding leads to a negative band at 1445 cm^{-1} (Fig. 3 *A*). It is small directly after the photolysis flash but increases in (negative) intensity with a rate constant of $k_{app} = 3.04\ s^{-1}$ (Fig. 2 *A*), until it reaches a constant value after ~1 s. The rate of ATP binding is very similar to the rate of ATP release, which implies that the rate of ATP binding to the Ca^{2+}-ATPase is limited by ATP release from caged ATP. Both reactions are complete after ~1 s.

Phosphorylation results in a positive band at 1720 cm^{-1} in the FTIR difference spectrum (Barth et al., 1996; Barth and Mäntele, 1998). This band is not observed with either AMP-PNP or ADP. Under the present conditions its amplitude is zero in the first 2 s after the photolysis flash but increases significantly afterward with an estimated rate constant of $k_{app} = 0.21\ s^{-1}$ (Fig. 2 *A*, fitting a single exponential to the data obtained after complete ATP release, i.e., after 1 s). Thus phosphorylation is more than 10-fold slower than ATP binding, and the state of ATP binding of

Ca_2E_1ATP is best observed between 1 and 2 s after the flash. During this interval ATP release and binding are almost complete, but Ca^{2+}-ATPase phosphorylation is still very low. Consequently, the 1720 cm^{-1} band is not observed in the ATP binding spectrum shown in Fig. 3 *A*. It should not be confused with the small 1716 cm^{-1} band observed in H_2O upon ATP binding (Fig. 3 *A*), which has a smaller amplitude and a different band position and is more strongly affected by deuteration.

In ^2H_2O only the phosphorylation reaction can be monitored at a marker band showing this partial reaction exclusively (Fig. 2 *B*). Two seconds after the flash a positive band at 1719 cm^{-1} starts to grow monoexponentially with a rate constant of $k_{app} = 0.18\ s^{-1}$. All other bands show a time dependency composed of two first-order reactions. As an example ATP binding and phosphorylation can be observed at the formation and subsequent partial decay of the band at 1663 cm^{-1} (Fig. 2 *b, filled squares*), which rises with a rate constant of $k_{app} = 7.15\ s^{-1}$ and partially decays with a rate constant of $k_{app} = 0.18\ s^{-1}$. The rate of the photolysis reaction in ^2H_2O was determined separately for samples without Ca^{2+}-ATPase. The decay of the band at 1470 cm^{-1} assigned to the vibration of the C═N bond of the aci-nitro intermediate (Barth et al., 1997) shows a rate constant of $k_{app} = 7.53\ s^{-1}$. Again, the rate of ATP binding to the ATPase seems to be determined by the rate of photolysis.

Difference spectra of the release of AMP-PNP or ADP in Ca^{2+}-ATPase samples show time-dependent changes only during the first second after the flash, which can be attributed to the photolysis reaction and to nucleotide binding. The Ca^{2+}-ATPase does not become phosphorylated to a significant extent by AMP-PNP, as judged by the lack of bands characteristic for phosphorylation (Barth et al., 1996), which is in line with previous observations (Taylor, 1981).

The rate of the photolytic release of ATP from caged ATP is higher in ^2H_2O than in H_2O. A primary isotope effect, which is caused by X-H bond cleavage, is unlikely to be the reason for the different rates, because it is expected to slow down the reaction by a factor between 6 and 8 in ^2H_2O (Conners, 1990; Isaacs, 1987). A factor of 0.5, as observed here, represents an inverse kinetic isotope effect and may be caused by a change in pK_A values of acidic residues in ^2H_2O affecting the H^+ catalysis of ATP release (Isaacs, 1987).

Infrared difference spectra of nucleotide release from caged derivatives

The photolysis of caged nucleotides in control samples without Ca^{2+}-ATPase results in FTIR difference spectra (*thin lines* in Figs. 3 and 4), which are discussed here briefly because they superimpose on the protein absorbance changes of Ca^{2+}-ATPase samples (*bold lines* in Figs. 3 and 4). Positive bands refer to the product of the reaction, while negative bands refer to the initial state of the educts. The

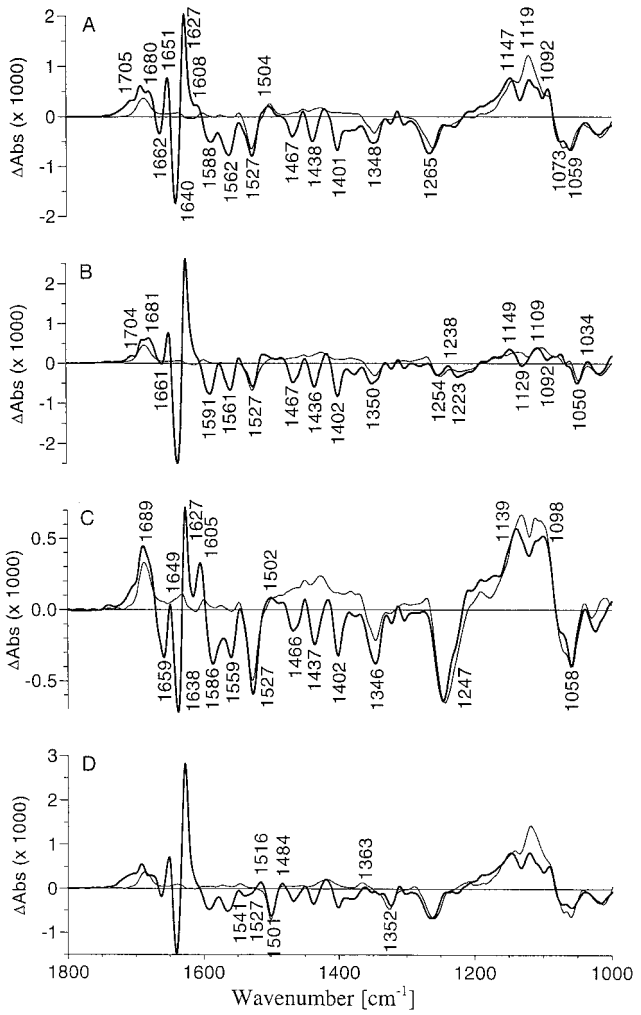

FIGURE 4 Infrared difference spectra upon nucleotide release in SR samples in ^2H_2O at −7°C. *Bold line*: Spectra of nucleotide release in SR samples, showing the nucleotide binding state. *Thin line*: Photolysis spectra of the caged nucleotide. Labels refer to the spectra of SR samples. (*A*) Difference spectra obtained in samples containing caged ATP. (*B*) Difference spectra obtained with caged AMP-PNP. (*C*) Difference spectra obtained with caged ADP. (*D*) Difference spectra obtained with [^{15}N]caged ATP.

band pattern of the ATP, ADP, and AMP-PNP photolysis spectra between 1800 and 1300 cm^{-1} are nearly identical because bands in this region are due to the 1-(2-nitro)-phenylethyl group of the caged nucleotide. The negative bands at 1525 and 1345 cm^{-1} have previously been assigned to the symmetrical and antisymmetrical stretching vibrations of the disappearing NO_2 group, and the positive band at 1688 cm^{-1} to the C═O group of the nitrosoacetophenone (Barth et al., 1991, 1995, 1997).

Bands in the region between 1300 and 900 cm^{-1} are dominated by changes of phosphate or P-O-P backbone vibrations. The transformation of the γ-PO_2^- group of caged ATP to the PO_3^{2-} group of free ATP is observed at 1254 and at 1120 cm^{-1} (Fig. 3 *A*). In the AMP-PNP

spectrum (Fig. 3 *B*), the influence of the NH group in AMP-PNP shifts the 1254 cm^{-1} band to 1244 cm^{-1}. From a comparison of spectra at pH 3, 7, and 11 in the region of ν_{as} PO_3^{2-} absorption we estimate that approximately two-thirds of the released AMP-PNP molecules are protonated at pH 7, whereas ATP is fully deprotonated (data not shown).

For [^{15}N]caged ATP, spectral shifts arise from the isotopic substitution (Fig. 3 *D*). The negative bands at 1527 and 1343 cm^{-1} of the antisymmetrical and symmetrical NO_2 vibrations of caged ATP are downshifted by 28 and 17 cm^{-1}, respectively (Barth et al., 1997). As described in Materials and Methods, this caged ATP isotope enabled us to correctly subtract the photolysis bands from the spectra of Ca^{2+}-ATPase samples recorded with unlabeled nucleotides. The resulting spectra are dominated by the effects of nucleotide binding to the Ca^{2+}-ATPase and are thus termed *nucleotide binding spectra*.

General comparison of the nucleotide binding spectra obtained with ATP, ADP, and AMP-PNP

Difference spectra of nucleotide release in Ca^{2+}-ATPase are shown in Fig. 3 for samples in H_2O and in Fig. 4 for samples in ^2H_2O, together with the photolysis spectra used for the subtraction of the photolysis bands. The band positions observed here are in excellent agreement with those observed in previous work (Barth et al., 1994, 1996), which were recorded at the higher temperature of 1°C in a different buffer.

Below 1300 cm^{-1}, bands assigned to the photolytic release of the nucleotides dominate the spectra of Ca^{2+}-ATPase samples, obscuring bands due to nucleotide binding in this region. Because small changes in the position or amplitude of a photolysis band may cause artificial bands in the subtraction procedure, we refrain from discussing bands of nucleotide binding spectra below 1300 cm^{-1}. Nucleotide binding spectra with compensated photolysis bands are shown in Fig. 5.

The nucleotide binding spectra of ATP and AMP-PNP agree very well between 1800 and 1300 cm^{-1} (Fig. 5, *A* and *B*). This is not surprising, because ATP and AMP-PNP are remarkably similar molecules in size and shape. The bond length and angles of the P-O-P and P-NH-P bridges between the β- and γ-phosphates are 1.63 Å and 128.7° for ATP and 1.68 Å and 127.2° for AMP-PNP (Yount et al., 1971; Larsen et al., 1969). With regard to the interactions of the bridging group, the proton of the imido group of AMP-PNP does not seem to interact with water molecules (Larsen et al., 1969). For ATP, quantum chemical calculations reveal only a slightly negative partial charge on the bridging oxygen, -0.12*e* to -0.17*e*, compared with -0.63*e* to -0.70*e* for the terminal oxygens of the γ-phosphate group (Saenger, 1984). Therefore, it seems unlikely that the bridging oxygen of diphosphates interacts strongly with polar or charged groups (King, 1994), and we think that strong interactions

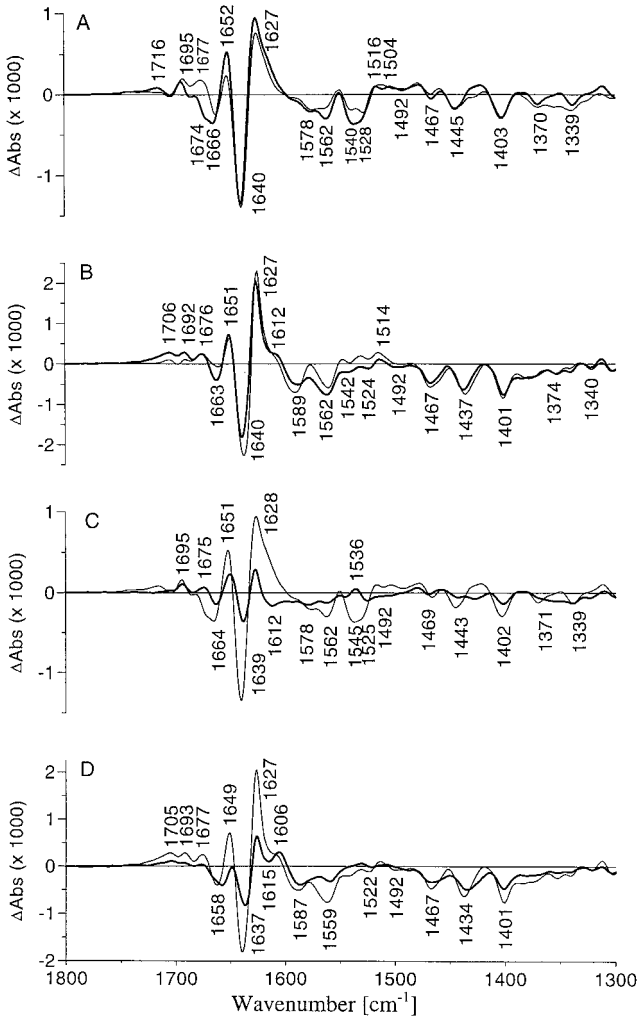

FIGURE 5 Nucleotide binding spectra (photolysis bands subtracted) at −7°C. Large labels refer to the bold line spectra, small labels refer to the thin line spectra. (*A*) H_2O; *bold line*: ATP; *thin line*: AMP-PNP. (*B*) ^2H_2O; *bold line*: ATP; *thin line*: AMP-PNP. (*C*) H_2O; *bold line*: ADP; *thin line*: ATP; (*D*) ^2H_2O; *bold line*: ADP; *thin line*: ATP.

of the Ca^{2+}-ATPase with the bridging groups of ATP and AMP-PNP are unlikely.

However, subtle differences (discussed below) between the ATP and AMP-PNP binding spectra are observed, which may be caused by the difference between ATP and AMP-PNP in their pK_a values (Klement et al., 1957; Yount et al., 1971). Under our conditions at pH 7.0, two-thirds of AMP-PNP molecules are protonated at the γ-phosphate, in contrast to ATP, which is completely deprotonated (see preceding section). We propose that the different protonation state of the γ-phosphate group is the reason for the subtle differences between the nucleotide binding spectra of ATP and AMP-PNP discussed below.

The nucleotide binding spectra of ATP and ADP also show similarities, with most of the bands present at the same position (Fig. 5, *C* and *D*). The most significant difference

between the ATP and ADP binding spectra is the amplitude of the bands. Despite the higher concentration of released ADP they are much smaller, which may be explained by incomplete binding of ADP to the ATPase. This would affect only the band amplitudes and not the band positions of the ADP binding spectrum. It is known that the affinity of Ca_2E_1 for ADP is ~10-fold lower than the affinity for ATP (Pickart and Jencks, 1984; Wakabayashi and Shigekawa, 1990). The dissociation constant for ADP binding was found to be in the 20–100-μM range, which would be sufficiently low to ensure saturating ADP binding in our experiments. Therefore we have to assume a higher dissociation constant of the ADP-ATPase complex under the conditions of concentrated infrared samples compared to the diluted samples used in the work cited above. This has been observed earlier under different conditions (Barth et al., 1994) and may be explained by a high ionic strength decreasing the affinity for ADP, as has been observed for the Na^+,K^+-ATPase (Nørby amd Esmann (1997). However, it was possible to obtain ADP-saturated ATPase under the previous conditions, and the amplitude of the bands was similar to the amplitude in the ATP binding spectrum observed here. Here the conditions for the ADP binding spectra were kept as close as possible to those of the ATP binding spectra, which were optimized for maximum observation time of Ca_2E_1ATP. Further differences between the ATP and the ADP binding spectrum are discussed below and arise because the γ-phosphate group is missing in ADP.

Changes of secondary structure

Binding of nucleotides leads to changes in the secondary structure of the Ca^{2+}-ATPase (Fig. 5). This is observed best at the intense signals between 1610 and 1700 cm^{-1}, which seem to be dominated by amide I modes, because there are only small shifts in ^2H_2O. Several discrete bands in the amide I range imply that different secondary structure elements are involved in nucleotide binding. The extent of net secondary structure change upon nucleotide binding is comparable to that of other partial reactions (Barth et al., 1996).

Without selective isotope labeling, it is difficult to localize the changes in secondary structure elements and attribute them to specific domains or residues. Because nucleotide binding changes the Ca^{2+} binding properties of the Ca^{2+}-ATPase (MacIntosh et al., 1996), it is possible that changes in the secondary structure upon nucleotide binding are not restricted to the nucleotide binding domain. Predictions of structure propose a mixture of alternating α-helices and β-strands in this domain (MacLennan et al., 1997). Changes in an α-helix structure may be the reason for the positive band at 1652 cm^{-1} (^2H_2O: 1651 cm^{-1}) and the negative sidebands in the ATP binding spectra (Fig. 5, *A* and *B*). The negative band at 1666 cm^{-1} (^2H_2O: 1663 cm^{-1}) can alternatively be caused by a conformational change in a turn structure. β-strands involved in ATP binding are likely to cause the bands at 1695 cm^{-1} (^2H_2O: 1692 cm^{-1}), 1640 cm^{-1}, and 1627 cm^{-1}.

The peak positions of most of the amide I bands in the AMP-PNP and ADP binding spectra are very similar to those of the ATP binding spectra. They are listed in Table 2 together with their tentative assignment. A difference between ATP and the other two nucleotides is observed near 1676 cm^{-1}. Here, all three nucleotide binding spectra show a positive band in ^2H_2O, which might be caused by a structural change in a turn structure. In H_2O, however, this band is observed only for AMP-PNP and ADP at a similar position but at 1682 cm^{-1} for ATP, most likely because of overlap of a negative band at 1674 cm^{-1}. This band seems to be characteristic of ATP binding and will be discussed below.

Many bands in the amide I region have a higher intensity in ^2H_2O, probably because small isotope shifts lead to less overlap in ^2H_2O between negative and positive bands of different peptide groups in this "crowded" spectral region.

In conclusion, the infrared absorbance changes in the amide I region give first-time evidence for changes in α-helix, β-sheet, and turn structure elements upon nucleotide binding. This is in general agreement with the predicted structure of the nucleotide binding domain (MacLennan et al., 1997; Møller et al., 1995).

The amide II vibration absorbs near 1550 cm^{-1} (Arrondo et al., 1993). Negative bands at 1540 and 1528 cm^{-1} are observed in the nucleotide binding spectra and can be assigned to amide II modes, because they are strongly reduced in ^2H_2O (Figs. 5, *A* and *B*). In the ^2H_2O spectra, only small bands remain at 1542 and 1524 cm^{-1}. A reason for these remaining bands could be an incomplete $^1H/^2H$ exchange of backbone protons deeply buried inside the protein. It can be excluded that an incomplete subtraction of the intense photolysis band at 1527 cm^{-1} is the reason for this feature, because these two bands are also seen in the spectra with samples containing [^{15}N]caged ATP (Fig. 4 *D*). An assignment of the 1528 cm^{-1} band to Lys is also possible and will be discussed below.

The negative 1540 cm^{-1} amide II band is not observed in the ADP binding spectrum (Fig. 5, *C* and *D*). Instead a small positive band at 1536 cm^{-1} is observed. The lack of the

TABLE 2 Band positions and tentative assignments in the amide I region

ATP		AMP-PNP		ADP		Tentative assignment
H_2O	^2H_2O	H_2O	^2H_2O	H_2O	^2H_2O	
1652	1651	1653	1651	1651	1649	α-helix
1695	1692	1693	1692	1695	1693	β-sheet
1640	1640	1640	1639	1639	1637	β-sheet
1627	1627	1626	1626	1628	1627	β-sheet
—	1676	1677	1677	1675	1677	turn
1666	1663	1664	1662	1664	1658	turn

1540 cm^{-1} band shows that some of the structural changes induced by ATP are not induced by ADP.

In ^2H_2O, the amide II′ mode of the polypeptide backbone appears near 1450 cm^{-1} (Arrondo et al., 1993), and we tentatively assign the negative band at 1437 cm^{-1} (1436 cm^{-1} for AMP-PNP) and most of the band intensity at 1467 cm^{-1} in the ^2H_2O ATP and AMP-PNP binding spectrum (Fig. 5 *B*) to this mode.

To summarise: absorbance changes in the amide I and II regions show that many of the secondary structure changes are observed for all three nucleotides tested, with ATP and AMP-PNP causing very similar changes to the Ca^{2+}-ATPase structure. However, differences have been observed between ATP and AMP-PNP binding on the one hand and ADP binding on the other. This points to an important role of the γ-phosphate in determining the conformation of the functional ATP-ATPase complex.

Individual amino acid side chains affected by nucleotide binding

Infrared difference spectra not only show changes in structure and hydrogen bonding of secondary structure elements but also reveal changes in the environment and protonation state of single amino acid side chains (Barth et al., 1996; Barth and Mäntele, 1998). A positive band at 1716 cm^{-1} in the ATP binding spectrum that shifts to 1706 cm^{-1} in ^2H_2O is readily assigned to the C═O mode of a protonated Asp or Glu residue (Fig. 5, *A* and *B*) (Venyaminov and Kalnin, 1990; Chirgadze et al., 1975). The spectra obtained with ADP and AMP-PNP show only the positive band at 1706 cm^{-1} (AMP-PNP) (1705 cm^{-1} for ADP) in ^2H_2O, but not the positive H_2O band at 1716 cm^{-1} (Fig. 5). This may indicate that the 1716 and 1706 cm^{-1} bands may not be caused by the same carboxyl group. Alternatively, a single group with a pK_a that is sensitive to the charge of the nucleotide and to $H/^2H$ exchange could cause both signals. Then the signals would be caused by the protonation of a carboxyl group induced by the negative charge of the phosphates. In ^2H_2O the less charged AMP-PNP (because it is protonated) and ADP induce protonation, as does ATP. In H_2O the pK_a value of carboxyl groups is generally lower than in ^2H_2O, and only the highly charged ATP molecule is able to increase the pK_a value sufficiently to induce protonation. For AMP-PNP and ADP the pK_S upshift is too small and the residue would still be deprotonated after nucleotide binding.

Deprotonated Asp and Glu residues absorb at 1574 and 1560 cm^{-1}, respectively (1584 and 1567 cm^{-1} in ^2H_2O), for the antisymmetrical stretching vibration and at 1402 (1405 in ^2H_2O) and 1404 cm^{-1} for the symmetrical stretching vibration (Venyaminov and Kalnin, 1990; Chirgadze et al., 1975). Deprotonated Glu or Asp side chains seem to participate in nucleotide binding because the negative bands at 1578, 1562, and 1403 cm^{-1} (^2H_2O: 1589, 1562, and 1401 cm^{-1}) can tentatively be assigned to those residues. The larger amplitude of the negative bands at 1589 and 1562 cm^{-1} in ^2H_2O as compared to H_2O is in line with the stronger absorption of ν_{as} CO_2^- in ^2H_2O and supports the assignment of these bands to carboxylate groups (Asp: ϵ (H_2O), 380 M^{-1} cm^{-1}; ϵ (^2H_2O), 820 M^{-1} cm^{-1}; Glu: ϵ (H_2O), 470 M^{-1} cm^{-1}; ϵ (^2H_2O), 830 M^{-1} cm^{-1}) (Venyaminov and Kalnin, 1990; Chirgadze et al., 1975).

In summary, there is a clear indication in the spectra that carboxyl groups are affected by nucleotide binding, owing to a change of environment and/or protonation, which seems to be caused by the charge of the phosphate groups.

The AMP-PNP and the ADP binding spectra show a positive band at 1677 cm^{-1}. In the ATP binding spectrum, the band is observed at 1682 cm^{-1} in H_2O. This shift seems to be caused by the overlap of an additional negative band at 1674 cm^{-1} in the ATP binding spectrum. In ^2H_2O only this 1674 cm^{-1} band shifts to smaller wavenumbers, revealing the "true" peak position of the positive band at 1676 cm^{-1}, as observed for AMP-PNP and ADP at 1677 cm^{-1}. Thus a negative band at 1674 cm^{-1} that is sensitive to $H/^2H$ exchange is observed only for ATP binding. There are two possibilities for an assignment of this band: 1) an amide I mode that shifts to 1663 cm^{-1} in ^2H_2O, where a negative band is observed with higher intensity for ATP than for AMP-PNP (Fig. 5 *B*); 2) the asymmetrical stretching mode of the Arg side chain, expected at 1673 cm^{-1} in H_2O and at 1608 cm^{-1} in ^2H_2O (Venyaminov and Kalnin, 1990; Chirgadze et al., 1975). Indeed in ^2H_2O at 1612 cm^{-1}, a shoulder possibly caused by a negative band is more pronounced in the ATP binding spectrum than in the AMP-PNP binding spectrum. Arginine is the only amino acid besides lysine with a positively charged side chain that can compensate for the negative charges of the phosphate groups of ATP. For that reason, Arg is frequently assumed to interact with the phosphate groups in different enzymes. Mutants of the Ca^{2+}-ATPase, where Arg^{489} is exchanged, show a significant change in ATPase activity (MacLennan et al., 1997; MacIntosh et al., 1996; Andersen, 1995).

In H_2O, the ATP and AMP-PNP binding spectra (Fig. 5 *A*) both show a positive band at 1516 cm^{-1} that shifts to 1514 cm^{-1} in ^2H_2O (Fig. 5 *B*). Band position and shift upon $H/^2H$ exchange are characteristic of a protonated Tyr residue (Venyaminov and Kalnin, 1990; Chirgadze et al., 1975; Takeuchi et al., 1988; Dollinger et al., 1986; Rothschild et al., 1986). In experiments with site-directed mutants, Tyr has not been discussed as a critical amino acid side chain for ATP binding. However, an interaction of a Tyr residue is conceivable because the Ca^{2+}-ATPase has several Tyr side chains in the nucleotide binding domain (Martonosi, 1992). An interaction of Tyr with the γ-phosphate group of GTP is observed in the crystal structure of the GTP binding site of the GTPase H-ras p21 (Pai et al., 1990). To summarize: we tentatively assign the band at 1516 cm^{-1} to a protonated Tyr residue.

The negative band at 1528 cm^{-1} may be assigned either to an amide II mode as discussed above or to the Lys NH_3^+ symmetrical deformation mode (Venyaminov and Kalnin, 1990). In line with both possible assignments, the band intensity is considerably reduced in ^2H_2O. Because of the positive charge of its side chain, Lys is a possible candidate for binding the negatively charged phosphate groups of ATP. Mutants of the SR Ca^{2+}-ATPase that lack Lys^{492} lose ~50% of their ATPase activity (MacLennan et al., 1997; Andersen, 1995). Lys^{515} is predicted to be close to the α- and β-phosphate groups, and mutations that replace this residue exhibit decreased Ca^{2+} transport activity (Martonosi, 1992; Clarke et al., 1990).

Band positions and relative amplitudes of the two negative bands at 1445 and 1339 cm^{-1} are in line with an assignment to the Trp side chain (Fabian et al., 1994; Lautie et al., 1980). Trp^{552} is the only Trp residue in the cytosolic domain C of the Ca^{2+}-ATPase (MacLennan et al., 1997). Experiments with a fragment of this domain (Asp^{351} to Arg^{615}) show fluorescence changes of this Trp residue upon nucleotide binding, indicating that the environment of this particular amino acid has changed (Champeil et al., 1998). Trp^{552} is predicted to be close to the adenine ring of bound ATP (MacLennan et al., 1997), and the aromatic rings of Trp might be a good partner for interaction with the purine of ATP. However tempting it may be, we refrain from assigning the negative bands at 1445 and 1339 cm^{-1} in the H_2O spectra to Trp^{552}, because it is possible that nucleotide binding leads to conformational changes apart from the nucleotide binding domain that affect one of the other 12 Trp residues.

In conclusion, the infrared spectra have revealed that protonated and unprotonated carboxyl group(s) and a protonated Tyr residue are affected by nucleotide binding. These residues have not been discussed so far in this context. Contributions of Arg, Lys, and Trp to nucleotide binding are also in line with the spectra.

Structural changes of ATP

ATP is the most preferred substrate for the Ca^{2+}-ATPase. Other triphosphate nucleotides are accepted, but the ATPase activity is decreased significantly (Inesi and de Meis, 1985). For this reason, the adenine ring of ATP is expected to interact with the Ca^{2+}-ATPase. Here we discuss signals in the ATP binding spectra that may be caused by the nucleoside moiety of ATP and exclude the phosphate modes because their signals are strongly disturbed by photolysis bands.

The strongest signal in an ATP absorbance spectrum above 1300 cm^{-1} is a band at 1660 cm^{-1}, which is assigned to the amino group of ATP (Tsuboi and Takahashi, 1973). Because of the strong overlap of amide I modes, a possible signal is not expected to be visible in the difference spectra. Other vibrations of purine have rather small extinction coefficients. Negative bands in the H_2O nucleotide binding spectra at 1492, 1370, and 1339 cm^{-1} might correspond to signals in the absorbance spectrum of ATP at 1480, 1378, and 1338 cm^{-1}. In an ATP absorbance spectrum in ^2H_2O, the 1378 and 1338 cm^{-1} bands are shifted upward to 1381 and 1341 cm^{-1}, while the 1480 cm^{-1} band remains at the same positions. The same behavior is observed in the ^2H_2O nucleotide binding spectrum, which shows negative bands at 1492 (no shift), 1374 (+4 cm^{-1}), and 1340 cm^{-1} (+ 1 cm^{-1}). The 1339 cm^{-1} band in H_2O may also be assigned to a Trp residue as discussed above.

Comparison with infrared difference spectra of other proteins

In the amide I region, which is sensitive to protein conformation, ATP and AMP-PNP binding to the Ca^{2+}-ATPase leads to six or seven difference bands in H_2O and ^2H_2O. So far, infrared difference spectra of nucleotide binding to three other proteins have been studied: GTP binding to H-ras P21 (Gerwert et al., 1993), ADP and ATP binding to creatine kinase (Raimbault et al., 1996), and arginine kinase in ^2H_2O (Raimbault et al., 1997). They often show bands at positions similar to those observed for the Ca^{2+}-ATPase, but the sign often differs. The number of bands corresponding in position and sign to those of ATP binding to the Ca^{2+}-ATPase is highest for GTP binding to H-ras P21, with three bands coinciding at 1671, 1629, and 1615 cm^{-1}. These positions are characteristic of β-sheet or turn structures. A band at 1639 cm^{-1} agrees in position but has the opposite sign, and three further bands do not agree in position. Thus there seem to be some similarities in the structural effects of nucleotide binding to the Ca^{2+}-ATPase and to H-ras P21, especially for β-sheet or turn structures. Loops often connected to β-strands undergo the principal interactions with the nucleotide in H-ras P21 (Wittinghofer and Pai, 1991). The correlation of band positions in the Ca^{2+}-ATPase nucleotide binding spectra seems to be better with creatine kinase and arginine kinase, with six bands coinciding. However, the sign of these bands is opposite those of the Ca^{2+}-ATPase for all of the bands of creatine kinase and for five bands in the 1630–1700 cm^{-1} region of ADP binding to the arginine kinase. Only the arginine kinase band at 1625–1628 cm^{-1} coincides in sign. Thus, while similar secondary structure elements seem to be affected by nucleotide binding to creatine kinase, arginine kinase, and the Ca^{2+}-ATPase, the effects of nucleotide binding to the two kinases seem to be largely opposite those of the Ca^{2+}-ATPase. In arginine kinase the nucleotide is bound close to β-sheet and loop structures (Zhou et al., 1998). For all three proteins the band at 1637–1639 cm^{-1} is positive, whereas the Ca^{2+}-ATPase band at 1640 is negative. This may point to an "unusual" structural rearrangement when ATP binds to the Ca^{2+}-ATPase.

CONCLUSIONS

Rapid-scan FTIR spectroscopy is able to monitor structural changes induced by the binding of molecules to an enzyme, even if this is a short-lived intermediate state. Nucleotide binding to the Ca^{2+}-ATPase leads to slight changes in secondary structure elements, with a distinctive contribution arising from the γ-phosphate group. Binding of the γ-phosphate also results in structural and environmental changes of single amino acid side chains. The charge on the γ-phosphate group seems to be important in the interaction with a carboxyl group. The environment of unprotonated carboxylate groups and of a protonated Tyr side chain changes upon nucleotide binding.

The authors acknowledge funding by the Deutsche Forschungsgemeinschaft (grant Ma 1054/10-3).

We thank Prof. Dr. W. Hasselbach (Max-Planck-Institut, Heidelberg) for the gift of Ca^{2+}-ATPase and Dr. J. E. T. Corrie (National Institute for Medical Research, London) for the preparation of caged AMP-PNP, caged ATP, and [^{15}N]caged ATP.

REFERENCES

Andersen, J. P. 1989. Monomer-oligomer equilibrium of sarcoplasmic reticulum Ca-ATPase and the role of subunit interaction in the Ca^{2+} pump mechanism. *Biochim. Biophys. Acta.* 988:47–72.

Andersen, J. P. 1995. Dissection of the functional domains of the sarcoplasmic reticulum Ca^{2+}-ATPase by site-directed mutagenesis. *Biosci. Rep.* 15:243–261.

Arrondo, J. L. R., A. Muga, J. Castresana, and F. M. Goni. 1993. Quantitative studies of the structure of proteins in solution by Fourier-transform infrared spectroscopy. *Prog. Biophys. Mol. Biol.* 59:23–56.

Barth, A., J. E. T. Corrie, M. J. Gradwell, Y. Maeda, W. Mäntele, T. Meier, and D. R. Trentham. 1997. Time-resolved infrared spectroscopy of intermediates and products from photolysis of 1-(2-nitrophenyl)ethyl phosphates: reaction of the 2-nitrosoacetophenone byproduct with thiols. *J. Am. Chem. Soc.* 119:4149–4159.

Barth, A., F. v. Germar, W. Kreutz, and W. Mäntele. 1996. Time-resolved infrared spectroscopy of the Ca^{2+}-ATPase. *J. Biol. Chem.* 271: 30637–30646.

Barth, A., K. Hauser, W. Mäntele, J. E. T. Corrie, and D. R. Trentham. 1995. Photochemical release of ATP from "caged ATP" studied by time-resolved infrared spectroscopy. *J. Am. Chem. Soc.* 117: 10311–10316.

Barth, A., and W. Mäntele. 1998. ATP induced phosphorylation of the sarcoplasmic reticulum Ca^{2+}-ATPase: molecular interpretation of infrared difference spectra. *Biophys. J.* 75:538–544.

Barth, A., W. Mäntele, and W. Kreutz. 1991. Infrared spectroscopic signals arising from ligand binding and conformational changes in the catalytic cycle of sarcoplasmic reticulum ATPase. *Biochim. Biophys. Acta.* 1057: 115–123.

Champeil, P., T. Menguy, S. Soulié, B. Juul, A. Gomez de Gracia, F. Rusconi, P. Falson, L. Denoroy, F. Henao, M. le Maire, and J. V. Møller. 1998. Characterization of a protease-resistant domain of the cytosolic portion of sarcoplasmic reticulum Ca^{2+}-ATPase. *J. Biol. Chem.* 273: 6619–6631.

Chirgadze, Y. N., O. V. Fedorov, and N. P. Trushina. 1975. Estimation of amino acid residue side-chain absorption in the infrared spectra of protein solutions in heavy water. *Biopolymers.* 14:679–694.

Clarke, D. M., T. W. Loo, and D. H. MacLennan. 1990. Functional consequences of alterations to amino acids located in the nucleotide binding domain of the Ca^{2+}-ATPase of sarcoplasmic reticulum. *J. Biol. Chem.* 265:22223–22227.

Conners, K. A. 1990. Kinetic isotope effects. *In* Chemical Kinetics: The Study of Reaction Rates in Solution. VCH, New York, Weinheim, Cambridge. 292–305.

de Meis, L., and W. Hasselbach. 1971. Acetyl phosphate as substrate for calcium uptake in skeletal muscle microsomes. *J. Biol. Chem.* 246: 4759–4763.

de Meis, L., and A. Vianna. 1979. Energy interconversion by the Ca-dependent ATPase of the sarcoplasmic reticulum. *Annu. Rev. Biochem.* 48:275–292.

Dollinger, G., L. Eisenstein, L. Shuo-Liang, K. Nakanishi, and J. Termini. 1986. Fourier transform infrared difference spectroscopy of bacteriorhodopsin and Ist photoproducts regenerated with deuterated tyrosine. *Biochemistry.* 25:6524–6533.

Fabian, H., C. Schultz, J. Backmann, U. Hahn, W. Saenger, H. H. Mantsch, and D. Naumann. 1994. Impact of point mutations on the structure and thermal stability of ribonuclease T1 in aqueous solution probed by Fourier transform infrared spectroscopy. *Biochemistry.* 33: 10725–10730.

Gerwert, K., V. Cepus, A. Scheidig, and R. S. Goody. 1993. Time-resolved FTIR studies of H-Ras P21 GTPase activity. *In* Proceedings of the Time-Resolved Vibrational Spectroscopy Congress. Springer-Verlag, Berlin.

Inesi, G., and L. de Meis. 1985. Kinetic regulation of catalytic and transport activities in sarcoplasmic reticulum ATPase. *In* The Enzymes of Biological Membranes, Vol. 3. A. N. Martonosi, editor. Plenum Press, New York. 157–191.

Isaacs, N. S. 1987. Kinetic isotope effects. *In* Physical Organic Chemistry. Longman, Harlow, UK. 255–281.

King, R. B. 1994. Encyclopedia of Inorganic Chemistry, Vol. 6. Wiley, New York. 3094.

Klement, R., G. Biberacher, and V. Hille. 1957. Beiträge zur Kenntnis der Monoamido- und Diamidophosphorsäure. *Z. Anorg. Chem.* 289:80–89.

Larsen, M., R. Willett, and R. G. Yount. 1969. Imidodiphosphate and pyrophosphate: possible biological significance of similar structures. *Science.* 166:1510–1511.

Lautie, A., M. F. Lautie, A. Gruger, and S. A. Fakhri. 1980. Etude par spectrométrie i. r. et Raman de l'indole et de l'indolizine. Liaison hydrogène NH$\cdots\pi$*. *Spectrochim. Acta.* A36:85–94.

MacIntosh, D. B., D. G. Woolley, B. Vilsen, and J. P. Andersen. 1996. Mutagenesis of segment ^{487}Phe-Ser-Arg-Asp-Arg-Lys^{492} of sarcoplasmic reticulum Ca^{2+}-ATPase produces pumps defective in ATP binding. *J. Biol. Chem.* 271:25778–25789.

MacLennan, D. H., W. J. Rice, and N. M. Green. 1997. The mechanism of Ca^{2+} transport by sarco(endo)plasmic reticulum Ca^{2+} ATPases. *J. Biol. Chem.* 272:28815–28818.

Martonosi, A. 1992. The Ca^{2+} transport ATPases of sarco(endo)plasmic reticulum and plasma membranes. *In* Molecular Aspects of Transport Proteins, Vol. 21. J. J. H. H. M. DePont, editor. Elsevier Science Publishers, Amsterdam. 57–116.

Møller, J. V., B. Juul, and M. le Maire. 1995. Structural organization, ion transport, and energy transduction of P-type ATPases. *Biochim. Biophys. Acta.* 1286:1–51.

Nørby, J. G., and M. Esmann. 1997. Nucleotide binding to Na,K-ATPase. Effect of ionic strength and charge. *Ann. NY Acad. Sci.* 834:410–411.

Pai, E. F., U. Krengel, G. A. Petsko, R. S. Goody, W. Kabsch, and A. Wittinghofer. 1990. Refined crystal structure of the triphosphate conformation of H-ras p21 at 1.35 Å resolution: implications for the mechanism of GTP hydrolysis. *EMBO J.* 9:2351–2359.

Pickart, C. M., and W. P. Jencks. 1984. Energetics of the calcium-transporting ATPase. *J. Biol. Chem.* 259:1629–1643.

Raimbault, C., F. Besson, and R. Buchet. 1997. Conformational changes of arginine kinase induced by photochemical release of nucleotides from caged nucleotides. An infrared difference-spectroscopy investigation. *Eur. J. Biochem.* 244:343–351.

Raimbault, C., R. Buchet, and C. Vial. 1996. Changes of creatine kinase secondary structure induced by the release of nucleotides from caged compounds. An infrared difference-spectroscopy study. *Eur. J. Biochem.* 240:134–142.

Rothschild, K. J., P. Roepe, P. L. Ahl, T. N. Earnest, R. A. Bogomolni, S. K. Das Gupta, C. M. Mulliken, and J. Herzfeld. 1986. Evidence for a tyrosine protonation change during the primary phototransition of bacteriorhodopsin at low temperature. *Proc. Natl. Acad. USA.* 83:347–351.

Saenger, W. 1984. Structures and conformational properties of bases, furanose sugars, and phosphate groups. *In* Principles of Nucleic Acid Structure. C. R. Cantor, editor. Springer-Verlag, New York, Berlin, Heidelberg, Tokyo. 51–104.

Takeuchi, H., N. Watanabe, and I. Harada. 1988. Vibrational spectra and normal coordinate analysis of p-cresol and ist deuterated analogs. *Spectrochim. Acta A.* 44:749–761.

Taylor, J. S. 1981. Sarcoplasmic reticulum ATPase catalyzes hydolysis of adenyl-5′-yl imidodiphosphate. *J. Biol. Chem.* 256:9793–9795.

Tsuboi, M., and S. Takahashi. 1973. Infrared and Raman spectra of nucleic acids—vibrations in the base-residues. *In* Physico-Chemical Properties of Nucleic Acids, Vol. II. J. Duchesne, editor. Academic Press, San Diego. 91–145.

Venyaminov, S. Y., and N. N. Kalnin. 1990. Quantitative IR spectrophotometry of peptide compounds in water (H_2O) solutions. I. Spectral parameters of amino acid residue absorption bands. *Biopolymers.* 30: 1243–1257.

Wakabayashi, S., and M. Shigekawa. 1990. Mechanism for activation of the 4-nitrobenzo-2-oxa-1,3-diazole-labeled sarcoplasmic reticulum ATPase by Ca^{2+} and its modulation by nucleotides. *Biochemistry.* 29: 7309–7318.

Wittinghofer, A., and E. F. Pai. 1991. The structure of Ras protein: a model for a universal molecular switch. *Trends Biochem. Sci.* 16:382–387.

Yount, R. G., D. Babcock, W. Ballantyne, and D. Ojala. 1971. Adenylyl imidodiphosphate, an adenosine triphosphate analog containing a P-N-P linkage. *Biochemistry.* 10:2484–2489.

Zhou, G., T. Somasundaram, E. Blanc, G. Parthasarathy, W. R. Ellington, and M. S. Chapman. 1998. Transition state structure of arginine kinase: implications for catalysis of bimolecular reactions. *Proc. Natl. Acad. Sci. USA.* 95:8449–8454.